Engineering Structures 174 (2018) 338–345

Contents lists available at ScienceDirect

Engineering Structures

journal homepage: www.elsevier.com/locate/engstruct

Enhancing the teaching of elastic buckling using additive manufacturing

Lawrence N. Virgin

School of Engineering, Duke University, Durham, NC 27708, USA

ARTICLE INFO

Keywords:
Buckling
Flexural stiffness
Thermoplastic
3D printing
Education

ABSTRACT

This is the third part in a trilogy of papers examining ways in which additive manufacturing can be used to facilitate the introduction of basic principles in structural analysis. Each paper uses 3D-printing and simple, but non-trivial, slender geometric forms, to provide a hands-on aspect to structural behavior in which flexure plays a dominant role. The first part dealt with linear structural analysis (Virgin, 2017), extended to dynamics and vibration in the second part (Virgin, 2017). The current paper focuses on slender structures in which compressive axial loading is the new ingredient and hence buckling becomes a central issue. This has similarities and differences with the two previous papers, but in all instances the role played by relatively high-precision 3D-printing opens the door to versatile and effective illustration, and the development of a deeper appreciation of structural phenomena.

1. Introduction

Buckling is almost always introduced using the pin-ended Euler strut. There are many reasons for this. It occupies a key position in the historical development of ordinary differential equations and their practical application. The pin-ends results in mathematical convenience, e.g., the zero bending moment at each end allows a model in the form of a second-order ordinary differential equation (rather than the more general fourth-order); an especially simple buckled mode shape (a half-sine wave); and conveniently forms the basis of effective length to incorporate other boundary conditions. However, there are a number of reasons why the modeling idealizations associated with pin-ended, purely axially-loaded, perfectly straight columns are relatively restrictive, including:

- sensitivity to geometry - most often encountered with a slight lack of straightness (initial geometric imperfection); a small lateral load (for example the effect of gravity in the case of a horizontal member); or an eccentricity in the application of the axial loading. No real structure is purely symmetric.
- boundary conditions that are intermediate between the standard cases, for example, when a column is part of a framework, and thus a specific column has a degree of elastic constraint at its ends.
- what happens after buckling? The linear theory only tells us that a non-trivial equilibrium configuration occurs at a critical point.

These effects are typically non-negligible in many applications of buckling, and in general conspire to make a linear eigenvalue analysis less useful when bending and buckling interact. The underlying Euler buckling problem is still useful as a fundamental concept and organizing center, but in this paper we seek to introduce an approach to buckling in which Euler buckling is introduced within the broader, more practical context of imperfect geometry and loading.

The capabilities of 3D-printing will be exploited to examine practical buckling issues, incorporating the three issues mentioned above with relatively precise geometry. A modular experimental set-up is described in which these effects can be examined in isolation or together, with the goal of providing a more comprehensive study than a typical introduction.

A number of standard analytical techniques will be used: solving the governing differential equations and using the matrix stiffness method, together with a simple approximate method, to verify the behavior observed in the testing of 3D-printed structures. The main emphasis (in similarity with the first two parts of this trilogy) is to illustrate the effect of geometry on buckling behavior. The direct comparison of theory and experiment depends on accurate measurements and appropriate values of Young's modulus etc., and although this paper includes some analysis for context, the important concept developed is how buckling is influenced by changes in geometry, boundary conditions and so on, in a *comparative* sense.

The use of simple physical buckling models is especially effective in the teaching realm, given the often sudden onset of buckling phenomena. The careful illustration of buckling using physical models was notably developed at University College London (UCL) and Northwestern University [3–5].

E-mail address: l.virgin@duke.edu.

https://doi.org/10.1016/j.engstruct.2018.07.059
Received 8 June 2018; Received in revised form 16 July 2018; Accepted 17 July 2018

2. Geometry of interest

2.1. Slenderness

For a structural element to suffer buckling it needs to be 'slender' and subjected to compressive axial loading, such that the system finds it easier to resist loading by a lateral deflection (orthogonal to the direction of loading) rather than a pure axial deformation [6,7]. A non-slender squat member will deform and fail in an axial sense, usually from material yielding. The conventional definition of what constitutes a slender column is given in terms of a slenderness ratio L/r, where L is the length (or effective length) of the member, and $r = \sqrt{I/A}$ is the radius of gyration. For a rectangular cross-section of width b and thickness d we have a second moment of area of $I = bd^3/12$, area $A = bd$, and thus $r = d/\sqrt{12}$, and $SR = L\sqrt{12}/d$. The distinction between squat and slender is not a clear-cut division (and many practical columns fall into this intermediate range), but it is generally recognized that an axially-loaded member would likely be susceptible to buckling if its slenderness ratio is greater than about 100. For the physical systems to be described later in this paper a typical geometry (in mm) might be $L \approx 100{-}115$, $b \approx 10{-}15$ and $d \approx 1{-}2$ and thus a SR ranging from about 200 to 400, and despite the effective length (to be described in detail later) often being a little smaller than the actual length we will be considering unambiguously *slender* structural members. And this slenderness range falls squarely within the size and resolution capabilities of most 3D-printers, even though 3D-printing is conventionally focused on components that are typically *not* slender or subjected to flexure.

2.2. A column with some end constraint

Based on the archetypal system to be described later, we develop a baseline model for a slender axially-loaded column with one end clamped and the other end pinned but with rotation constrained by a torsional spring [8–14]. This is shown schematically in Fig. 1. The column has length L, flexural rigidity EI, a rotational spring at the right end of coefficient C (and later to be associated with the influence of adjacent structural members). Subjected to an axial force P we seek the behavior of the lateral deflection $W(x)$, specifically where its rate of increase grows rapidly: buckling. As mentioned in the introduction, in addition to the elastic constraint at the boundary, we will also incorporate an initial geometric imperfection in the form of a non-flat shape (shown exaggerated in part (b)), and an eccentric point of application ϵ of the axial load P. Both of these apparently minor effects are quite typical in practice, and destroy the symmetry of the system [16,17].

One of the useful pedagogical aspects of this system is that the anticipated buckling behavior is bracketed by extreme cases: when the torsional spring is very weak, i.e., $C \to 0$, we expect buckling close to the clamped-pinned case ($P_{cr} \to 2EI(\pi/L)^2$), and when the torsional spring is very stiff, i.e., $C \to \infty$, we expect the clamped-clamped case ($P_{cr} \to 4EI(\pi/L)^2$).

We shall focus on a number of techniques of varying degrees of utility in buckling analysis ranging from the classical differential approach to matrix structural analysis. Within this range are a variety of energy-based, Rayleigh-Ritz approaches but we shall not focus on these in the current paper.

2.3. The classical approach

Based on Euler-Bernoulli beam theory, the governing equation for the initially flat, axially-loaded column is given by [7,21]

$$EI\frac{d^4W(X)}{dX^4} + P\frac{d^2W(X)}{dX^2} = 0, \tag{1}$$

subject to the boundary conditions: for clamped at $X = 0$ we require $W(0) = 0$ and $dW(0)/dX = 0$, and for elastic rotational constraint at $X = L$ we have $W(L) = 0$ and $EI[d^2W(L)/dX^2] + C[dW(L)/dX] = 0$. It is convenient to nondimensionalize using $w = W/L; x = X/L; p^2 = PL^2/EI; \lambda = CL/EI$ to obtain:

$$w'''' + p^2w'' = 0, \tag{2}$$

where a prime denotes differentiation with respect to x, and the boundary conditions become: $w(0) = 0$ and $w'(0) = 0$ at $x = 0$; and $w(1) = 0$ and $w''(1) + \lambda w'(1) = 0$ at $x = 1$.

The general form of the solution to Eq. (2) is

$$w = -A/p^2\sin(px) - B/p^2\cos(px) + Cx + D, \tag{3}$$

and applying the boundary conditions leads to:

$$\begin{bmatrix} 0 & -1/p^2 & 0 & 1 \\ -1/p & 0 & 1 & 0 \\ -1/p^2\sin p & -1/p^2\cos p & 1 & 1 \\ (\sin p - \lambda/p\cos p) & (\cos p + \lambda/p\sin p) & \lambda & 0 \end{bmatrix} \begin{bmatrix} A \\ B \\ C \\ D \end{bmatrix} = \begin{bmatrix} 0 \\ 0 \\ 0 \\ 0 \end{bmatrix} \tag{4}$$

Setting the determinant equal to zero for non-trivial solutions leads to a characteristic equation with a lowest root $p(\lambda)$ corresponding to buckling. This relation is shown in Fig. 2, in which we see the two extremes: clamped-pinned, $p_{cr} \to 2\pi^2$; clamped-clamped, $p_{cr} \to 4\pi^2$.

2.3.1. Effective length

Given the central role played by the Euler buckling load for a pinned-pinned column ($P_{cr} = EI(\pi/L)^2$) it is natural to relate other boundary conditions back to this case. A physical motivation for doing this is that the buckling of a column with various boundary conditions can be envisioned as subsuming a pin-ended column in which the length is taken as the distance between points of inflection (where the bending moment is zero) - the effective length L_e. The effective length for a clamped-clamped column is $L_e = 0.5L$ and for a clamped-pinned column is $L_e \approx 0.7L$, and plugging these value into the Euler expression furnishes the values at the extreme ranges of the column with some elastic torsional end constraint.

2.3.2. Buckling mode shapes

The buckled mode shape is found by eliminating B, C and D from Eq. (4) to give

$$w = -A/p^2\left[px - \sin(px) + \frac{(p - \sin p)}{(\cos p - 1)}(1 - \cos(px))\right], \tag{5}$$

in which A is arbitrary, and p is obtained from the determinant for a given λ. For example, Fig. 3 shows the buckling mode shapes for $\lambda = 0$ and 60, in which the latter is practically the clamped-clamped mode shape. By setting the second derivative of the mode shape equal to zero we can find the points of inflection and the distance between them gives

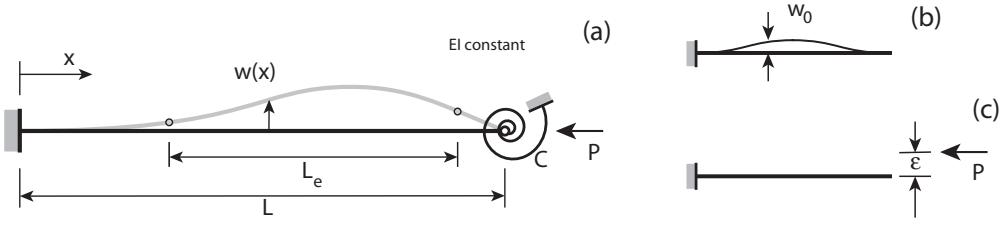

Fig. 1. (a) A schematic of an axially-loaded column, with rotational elastic constraint at one end, (b) with a small initial deflection, (c) with a small axial load eccentricity.